A Comparative Study and Evaluation on Several Typical Iterative Methods for Bioluminescence Tomography

Liu Hejuan Hou Yuqing He Xiaowei Pu Xin

School of Information and Technology, Northwest University, Xi'an, Shaanxi 710127, *China*

Abstract Bioluminescence tomography (BLT) has recently emerged as a promising preclinical imaging modality. Iterative methods based on sparse regularization play a critical role in solving the ill-posed BLT inverse problem. Four kinds of typical iterative methods based on l_1 regularization were briefly introduced and applied to reconstruct the bioluminescent source location and intensity, which include interior-point methods, homotopy methods, first-order methods, and augmented Lagrangian methods. Numerical experiments on a digital inhomogeneous mouse model and *in vivo* experiments were conducted to evaluate the performance of these methods in terms of localization accuracy, reconstructed intensity and power.

Key words medical optics; bioluminescence tomography; source reconstruction; iterative algorithm; l_1 regularization

OCIS codes 170.3010; 170.6960; 170.6280

几种典型迭代算法在生物发光断层成像中的对比研究及评估

刘合娟 侯榆青 贺小伟* 蒲 鑫

西北大学信息科学与技术学院, 陕西 西安 710127

摘要 生物发光断层成像是一种新型光学分子影像技术。基于稀疏正则化的迭代算法在解决重建中病态问题起着关键的作用。将4种典型的基于l_1正则化的迭代算法(内点法、同伦算法、一阶方法和拉格朗日算法)应用于重建过程中,分别进行数学推导,并从重建精度和重建速度方面进行了实验对比和性能评估。实验结果表明尽管4种方法均能较好地重建出光源位置,但时间代价和重建能量大小上存在差异,据此结果为不同情况下重建算法的选取提出建议。

关键词 医用光学; 生物发光断层成像; 光源重建; 迭代算法; l_1正则化

中图分类号 TP391; Q63 **文献标识码** A

doi: 10.3788/LOP52.081704

1 Introduction

Bioluminescence tomography (BLT) is a new optical molecular imaging technique with the features of high detection sensitivity, relatively low cost and easy use, *etc.*, and it has recently emerged as a promising tool in oncology, metastasis monitoring and drug development[1-3].

As an important modality in optical molecular imaging, BLT problem involves forward and inverse problem. The forward problem investigates the light propagation in biological tissues, which is the basis and prerequisite for the inverse problem. The inverse problem aims to reconstruct internal bioluminescent source from the photon density measured on the tissue surface. The light propagation in biological tissues is influenced by various factors such as scattering and absorption[4], which makes the intensity on the surface

收稿日期: 2015-02-17; **收到修改稿日期**: 2015-04-09; **网络出版日期**: 2015-07-21

基金项目: 国家自然科学基金(61372046)

作者简介: 刘合娟(1989—),女,硕士研究生,主要从事医学图像处理方面的研究。E-mail: liuhejuan012@126.com

导师简介: 侯榆青(1963—),女,教授,主要从事信号处理、医学图像处理、DSP应用技术等方面的研究。E-mail: houyuqin@nwu.edu.cn

*通信联系人。E-mail: hexw@nwu.edu.cn

greatly reduced and brings difficulty to locate the bioluminescent source in BLT.

Two challenging problems facing the reconstruction algorithm are the severe ill-posedness of BLT inverse problem, and the large-scale numerical problem involved in tomographic imaging. Wang *et al.*[5] combine anatomical structure and optical parameters as priori information to alleviate the ill-posedness of the problem. Cong *et al.*[6] adopt a priori permissible source region-based reconstruction method to obtain stable reconstruction. Lv *et al.*[7] develop a multi-level adaptive finite element algorithm for BLT, which helps improve source localization and quantification. Jiang *et al.*[8] implement the source reconstruction from part of the measurement data by expectation maximization (EM) method and constraint Landweber iterative method. In view of the spectral characteristics of the underlying bioluminescence source, Chaudhari *et al.*[9] develop multispectral and hyperspectral methods, which have improved the reconstruction accuracy and detecting depth. As shown in reference [10], reconstruction algorithm is the key of successful BLT application.

Regularization is a common technique adopted in most reconstruction algorithms to deal with the ill-posedness of BLT. As a typical l_2 regularization method, Tikhonov regularization is widely used in BLT reconstruction[11]. However, due to the inherent characteristic of Tikhonov regularization, these methods usually produce smooth solutions which will result in the loss of high frequency parts and lower accuracy of localization. In BLT applications, bioluminescent probes and gene reporters are associated with target specific biological tissues, which are typically sparse. The sparsity-seeking property of l_1 norm based optimization has been shown in many signal processing areas. In BLT, l_1 regularization based reconstruction algorithms tend to gain high quality reconstruction images from insufficient boundary measurement. Therefore, l_1 regularization has attracted much attention in BLT reconstruction. A number of algorithms based on l_1 regularization have recently been proposed for 3D bioluminescence reconstruction[12-15].

In this research, four kinds of commonly used iterative regularization methods are investigated and applied to reconstruct the bioluminescent source location and intensity. They are interior-point methods (PDIPA and L1LS)[16], homotopy algorithm (homotopy)[17], first-order methods (FISTA)[18], and augmented Lagrangian algorithm (PALM and its dual algorithm DALM)[19]. The purpose of this study is to investigate the performance of these iterative regularization methods in BLT.

2 Methods

2.1 Reconstruction model for BLT

The diffusion approximation model of radiative transfer equation (RTE) is applied to reconstruct the bioluminescent source location and intensity[20]. By solving the diffusion equations with finite element method, we can establish the linear relationship between the boundary measurement $\boldsymbol{b}\in R^m$ and the internal source distribution $x\in R^n$ [21].

$$\boldsymbol{A}x=\boldsymbol{b}\ , \tag{1}$$

where $\boldsymbol{A}\in R^{m\times n}$ $(m\ll n)$ is a weighting matrix, relating the measurement to the unknowns. However, the unknown source distribution cannot be obtained by direct solving of Eq. (1) due to the high ill-posedness of BLT. Based on priori information of source distribution, the BLT problem is converted to the following l_1-norm minimization problem or an equivalent l_1-norm regularized minimization problem.

$$\min_x \|x\|_1 \quad \text{s.t. } \boldsymbol{A}x=\boldsymbol{b}\ , \tag{2}$$

or

$$F(x)=\min_x \frac{1}{2}\|\boldsymbol{A}x-\boldsymbol{b}\|_2^2+\lambda\|x\|_1\ , \tag{3}$$

where $\|x\|_1$ is an sparse-inducing regularizer to stable the solution λ is the regularizaton parameter. By solving Eq. (3) with an appropriate optimization method, we can achieve accurate approximation for the source distribution from limited boundary measurement.

2.2 Iterative reconstruction algorithms

We consider four groups of iterative reconstruction algorithms to solve the Eq. (3).

2.2.1 Interior-point methods

Primal-dual interior-point algorithm (PDIPA) is considered as a classical approach to solve l_1-norm minimization problems. Considering the actual intensity of bioluminescence source is nonnegative, the Eq. (3) can be rewritten as a linear programming (LP):

$$\begin{array}{ll} \text{primal (P)} & \text{dual (D)} \\ \min\limits_{x} \quad 1^{\mathrm{T}}x; & \max\limits_{y,z} \quad \boldsymbol{b}^{\mathrm{T}}y. \\ \text{s.t.} \quad \boldsymbol{A}x=\boldsymbol{b} \quad , & \text{s.t.} \quad \boldsymbol{A}^{\mathrm{T}}y+z=1 \quad . \\ \quad x\geqslant 0 & \quad z\geqslant 0 \end{array} \tag{4}$$

The basic idea of primal-dual interior-point method is to formulate the inequality constrained Eq. (4) as an equality constrained problem, which can be solved by the barrier method. As a classical method, PDIPA has been applied in the BLT[15]. However, the complexity of PDIPA is dominated by the Newton update step, which is computationally expensive for large l_1- min problems. Hence, an improved interior-point method can be used to approximate its solution, which is the truncated Newton interior-point method (TNIPM), also known as L1LS[22].

L1LS solves an optimization problem of the Eq. (3). It transforms the objective function of Eq. (2) into a quadratic programming with inequality constraints,

$$\min \frac{1}{2}\left\|\boldsymbol{A}x-\boldsymbol{b}\right\|_2^2+\lambda\sum\nolimits_{i=1}^{n}v_i \ , \ \text{s.t.}\ -v_i\leqslant x_i\leqslant v_i, \ i=1,2,...,n \ . \tag{5}$$

Then define a logarithmic barrier for the bound constraints $-v_i\leqslant x_i\leqslant v_i$ in Eq. (5):

$$\Phi(x,v)=-\sum\log(v_i+x_i)-\sum_i\log(v_i-x_i). \tag{6}$$

The central path consists of the unique minimized variable $\left[x^*(t),v^*(t)\right]$ of the convex function

$$F(x,v)\equiv t\left(\left\|\boldsymbol{A}x-\boldsymbol{b}\right\|_2^2+\lambda\sum_{i=1}^{n}v_i\right)+\Phi(x,v) \ , \tag{7}$$

where the parameter t changes from 0 to ∞. Different from primal barrier method, the search direction is computed by a truncated Newton method[23].

2.2.2 Homotopy method

The basic idea of the homotopy algorithm is as follows: in solving the basic pursuit problem of noisy background in Eq. (3), along with the decrease of λ, the objective function $F(x)$ undergoes homotopy from the l_2 constraint to the l_1 objective, *i.e.* when $\lambda\to\infty$, $x_\lambda^*=0$; when $\lambda\to 0$, x_λ^* converges to the solution of Eq. (1). Taking the subdifferential of $\left\|x\right\|_1$ into account, it can be defined as follows:

$$w(x)\overset{\Delta}{=}\partial\left\|x\right\|_1=\left\{w\in R^n:\begin{array}{l} w_i=\operatorname{sgn}(x_i), \ x_i\neq 0 \\ w_i\in[-1,1], \ x_i=0 \end{array}\right\}. \tag{8}$$

The homotopy algorithm runs iteratively, initial $x^{(0)}=0$. In each iteration of a non-zero λ, $0\in\partial F(x)$ can be used to make $c(x)=\boldsymbol{A}^{\mathrm{T}}\boldsymbol{b}-\boldsymbol{A}^{\mathrm{T}}\boldsymbol{A}x\in\lambda w(x)$.

According to the definition in Eq. (8), in the first k iteration, we maintain a sparse support set $I=\left\{i:\left|c_i^k(x)\right|=\lambda\right\}$. The algorithm is then only to calculate the update direction and step for the non-zero coefficients of $x^{(k)}$ which is identified by I. Since the update only involves the non-zero coefficients in I, and when x is sparse it can be very small, the computational cost of homotopy algorithm can be greatly improved from the interior-point methods.

2.2.3 First-order methods

In the optimization, first- order methods refer to those algorithms which use the structure of the

subdifferential of the $\|\cdot\|_1$. There are many first-order methods in recent years, such as proximal-point methods, parallel coordinate descent, approximate message passing. Here we consider a typical algorithm, namely fast iterative soft-thresholding algorithm (FISTA), which has a significantly better convergence rate.

First we define a proximal operator of a convex function g of $x \in R^n$ as

$$f_{\text{prox}g}(x) = \arg\min_u g(u) + \frac{1}{2}\|u - x\|_2^2, \tag{9}$$

where $g(x) = \alpha\|x\|_1$, and the proximal operator can turn into closed-form expression which is called the soft-thresholding or shrinkage operator:

$$f_{\text{soft}}(x,\alpha)_i = f_{\text{sign}}(x_i) \cdot \max\{|x_i| - \alpha, 0\},\ i = 1,2,\cdots,n. \tag{10}$$

The key idea behind FISTA is that, instead of forming a quadratic approximation of Eq. (3) at x_k at the k-th iteration, it uses a more carefully chosen sequence y_k, the details are described as follows:

$$x_k = f_{\text{soft}}\left[y_k - \frac{1}{L_f}\nabla f(y_k), \frac{\lambda}{L_f}\right],\ t_{k+1} = \frac{1+\sqrt{1+4t_k^2}}{2},\ y_{k+1} = x_k + \frac{t_k - 1}{t_{k+1}}(x_k - x_{k-1}), \tag{11}$$

where $y_1 = x_0$ and $t_1 = 1$. Define that $g(x) = \|x\|_1$, and $f(x) = \frac{1}{2}\|\boldsymbol{A}x - \boldsymbol{b}\|_2^2$. $\nabla f(x) = \boldsymbol{A}^{\mathrm{T}}(\boldsymbol{A}x - \boldsymbol{b})$ is Lipschitz continuous with Lipschitz constant $L_f = \|\boldsymbol{A}\|^{24}$. Thus, we have a slightly different problem whose solution gets closer to the solution set of Eq. (1) as $\lambda \to 0$.

2.2.4 Augmented Lagrangian method (ALM)

Augmented Lagrangian method (ALM) is a special class of first-order method, which uses a Lagrange multiplier in l_1-min problems. Applying ALM to the primal problems, we can get the complete ALM algorithm which is the primal ALM (PALM) for solving the primal l_1-min problem, while DALM is the method that applies ALM to the dual problems. Because the solving steps are different, the computational time is also different for PALM and DALM. Generally the DALM is the preferred method. Assume $p(x) = \|x\|_1$, and $h(x) = b - Ax$. Because p and h are continuous convex functions of x, we can assume that Eq. (1) has a unique global minimum. Therefore, for any $\xi > 0$, we modify cost function and Eq. (1) has the same optimal solution x^* accompanied with additional penalty term,

$$\min_x p(x) + \frac{\xi}{2}\|h(x)\|_2^2 \qquad \text{s.t.} \quad h(x) = 0. \tag{12}$$

Although other penalty functions can also be used, secondary is preferred because of its smoothness. Lagrangian operator of the Eq. (11) is given by

$$L_\xi(x,\theta) = p(x) + \frac{\xi}{2}\|h(x)\|_2^2 + \theta^{\mathrm{T}}h(x), \tag{13}$$

where $\theta \in \Re^m$ is a vector of Lagrange multipliers, $L_\xi(.,.)$ is called the augmented Lagrange multiplier of Eq. (1)[24]. There exists $\xi^* \in \Re^m$ (which is not the only one) and $\xi^* \in \Re$ to make

$$x^* = \arg\min L_\xi(x,\theta^*), \forall \xi > \xi^*. \tag{14}$$

Therefore, by minimizing augmented Lagrangian function operator $L_\xi(x,\theta)$, we can find the optimal solution of Eq. (1). Using multiplier method, Eq. (14) can be solved by constructing an iteration,

$$\begin{cases} x_{k+1} = \arg\min_x L_{\xi_k}(x,\theta_k) \\ \theta_{k+1} = \theta_k + \xi_k h(x_{k+1}) \end{cases}. \tag{15}$$

where $\{\xi_k\}$ is a predefined sequence.

While we used the augmented Lagrangian principle in the dual problem of Eq. (1), it can be represented as follows:

$$\max \boldsymbol{b}^{\mathrm{T}}y \qquad \text{s.t.} \quad \boldsymbol{A}^{\mathrm{T}}y \in B_1^\infty \quad , \ B_1^\infty = \left\{x \in R^n : \|x\|_\infty \leqslant 1\right\}. \tag{16}$$

The corresponding Lagrangian function is given by the following equation:

$$\min_{y,z} -\boldsymbol{b}^{\mathrm{T}}y - x^{\mathrm{T}}\left(z-\boldsymbol{A}^{\mathrm{T}}y\right)+\frac{\beta}{2}\left\|z-\boldsymbol{A}^{\mathrm{T}}y\right\|_2^2,\ \text{s.t.}\quad z\in B_1^{\infty}. \tag{17}$$

The problem about y, x and z is difficult, so we take alternate strategy, while in the process of hidden variable, iterative minimization of the cost function with another variable. Given (x_k, y_k), the minimizer z_{k+1} which respects to z is given by

$$z_{k+1}=p_{B_1^{\infty}}\left(\boldsymbol{A}^{\mathrm{T}}y_k+x_k/\beta\right), \tag{18}$$

where $p_{B_1^{\infty}}$ represents the projective operator to B_1^{∞}. Given (x_k, z_{k+1}), minimization of y is a least squares problem. Its solution is obtained by solving the equation:

$$\beta\boldsymbol{A}\boldsymbol{A}^{\mathrm{T}}y=\beta\boldsymbol{A}z_{i+1}-\left(\boldsymbol{A}x_i-\boldsymbol{b}\right). \tag{19}$$

Assume that $\boldsymbol{A}\boldsymbol{A}^{\mathrm{T}}$ is invertible, Eq. (19) can be solved directly.

3 Experiments and results

3.1 Comparison of convergence rate

We compared the time cost of the four methods for solving the problem in Eq. (1). We constructed a detection matrix $\boldsymbol{A}$ with size of $m\times n(m<n)$, and insured that every input matrix was independent and with identical Gaussian distribution. The observables b can be calculated from the X, x_0 is a sparse vector, its selection is random. Its non-zero input is independent and identically distributed, uniformly distributed in the range [−10, 10]. Assume d is the sparseness of x_0, *i.e.* $\|x_0\|_0=d$. Providing m=800, for different n and d, we estimated the relative error and calculating time of x_0. Fig. 1 shows the average relative error after 5 iterations.

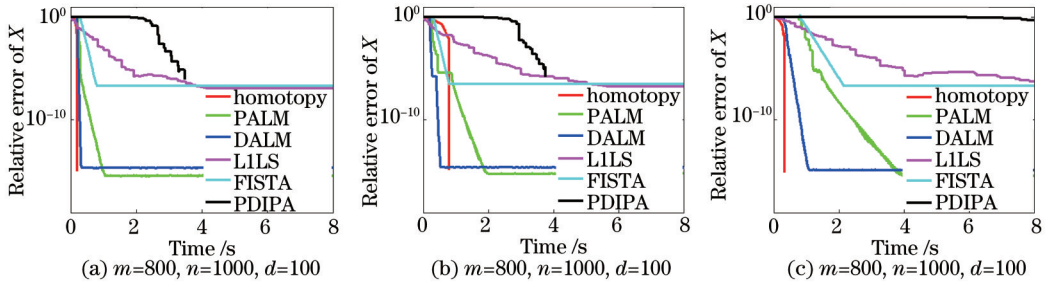

Fig.1 Time cost and calculation accuracy of each algorithm

From Fig. 1, we can find that DALM is the fastest algorithm in all the cases. ALM and homotopy algorithm can achieve near-machine precision $\left[r_k(x)\leqslant 10^{-10}\right]$ in solving the problem. We find that the homotopy algorithm is very sensitive to the sparseness d. When the number of unknowns increases, the speed of all these algorithms will slow down, especially for homotopy. However, under the same sparseness, homotopy is not sensitive to unknowns n. PDIPA is the most sensitive algorithm to the size of the problem, and produces the largest relative error in all cases; hence it is not suitable for large scale data problems. Overall, compared to the primal algorithms (PDIPA, L1LS, FISTA and PALM), the dual algorithm DALM is less sensitive to n.

3.2 Digital mouse experiment

In order to assess the performance of these typical iterative algorithms in bioluminescence tomography, a digital mouse model is used for testing, as shown in Fig. 2[13]. Five major organs of the mouse are considered, including heart, lungs, liver, kidneys and stomach. The optical parameters are given in table 1[6]. In the experiment, the digital mouse model was discretized to a finite mesh with 112795 elements and 21277 nodes. The mouse model was implanted with a cylindrical light source with 0.5 mm radius and 1.0 mm height. The true light source was located in the liver, and its coordinates were (18.1 mm, 6.3 mm, 15.4 mm). The total power and power density were initialized as 0.785 nW and 1 nW/mm^3 respectively.

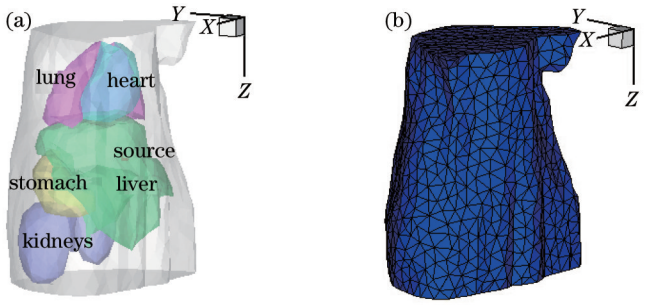

Fig.2 Digital mouse model. (a) 3D mouse model with a light source in the liver; (b) 3D mesh

Table 1 Optical parameters for the non-homogeneous phantom

Organ	μ_a /mm^{-1}	μ_s /mm^{-1}
Heart	0.0104	0.99
Lung	0.0203	1.95
Liver	0.0176	0.65
Kidney	0.0380	2.02
Stomach	0.0070	1.36

The above four kinds of algorithms are performed to recover the BLT source and the corresponding results are shown in Fig. 3. Table 2 presents the specific quantitative results.

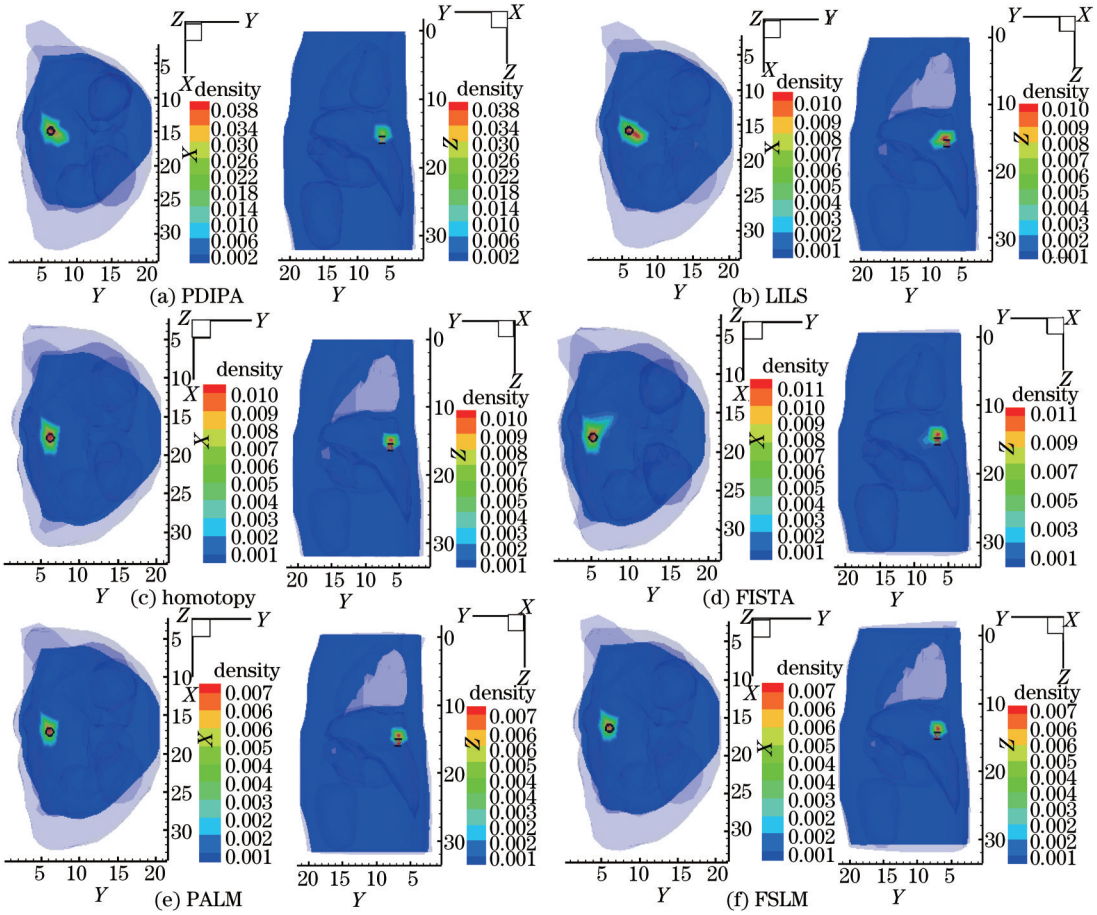

Fig.3 Reconstruction results of each algorithm

From table 2, we can find that the reconstructed power by PDIPA, homotopy and L1LS is higher than that of others, while PALM, DALM and homotopy have lower location error (LE). In general, homotopy algorithm makes good performance in all the evaluated indexes.

Table 2 Contrast of the digital mouse experimental data

Iterative method	Power density /(nW/mm^3)	Total power /nW	Reconstruction location /mm	LE /mm
PDIPA	0.0390	0.4106	(17.31 7.79 12.42)	3.51
L1LS	0.0106	0.1120	(18.96 7.63 15.54)	1.59
Homotopy	0.0115	0.1215	(17.85 6.22 14.85)	0.61
FISTA	0.0051	0.0533	(16.97 7.89 15.81)	1.99
PALM	0.0075	0.0786	(17.93 6.22 14.86)	0.57
DALM	0.0094	0.0993	(17.92 6.22 14.94)	0.50

3.3 *In vivo* experiment

The *in vivo* experiments were presented here to compare the performance of various methods for mouse applications. A catheter containing luminescent liquid was implanted into a living mouse as the test source. The mouse torso section was scanned using micro-CT (computer tomography) and segmented into major anatomical components, including muscle, heart, liver, lungs and kidneys, as shown in Fig. 4. The optical parameters of each organ are listed in table 3[25]. The center coordinates of the light source were (21 mm, 27.4 mm, 9.4 mm). The model was discretized into 3170 nodes and 15086 tetrahedral elements. The reconstruction results are shown in Fig. 5, and table 4 presents the specific quantitative results.

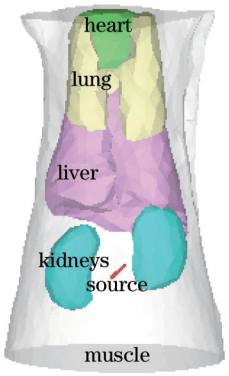

Fig.4 Torso model of the real mouse with one source

Table 3 Optical parameters for the mouse organs

Organ	μ_a /mm^{-1}	μ_s /mm^{-1}
Heart	0.14	1.08
Lung	0.46	2.27
Liver	0.82	0.74
Kidney	0.15	2.53
Muscle	0.01	1.26

Table 4 Contrast of the *in vivo* experimental data

Iterative method	Power density /(nW/mm^3)	Reconstruction location /mm	LE /mm
PDIPA	0.5100	(18.35 26.44 11.55)	3.552
L1LS	0.1351	(19.98 29.40 10.87)	2.686
Homotopy	0.1592	(19.89 28.91 10.75)	2.313
FISTA	0.1065	(18.60 27.13 11.86)	3.447
PALM	0.0976	(20.20 30.09 10.95)	3.204
DALM	0.1592	(19.90 28.91 10.75)	2.309

From the table 4 and Fig. 5, we find that all the reconstruction results of the real mouse experiments are not better than the digital mouse experiments, but the overall trend is consistent. For example, DALM shows the best performance, and the performance of PDIPA is the worst. Therefore, the LE of the individual method increases greatly as the PALM, the possible reason is that the method is not robust to the noise in the *in vivo* experiments.

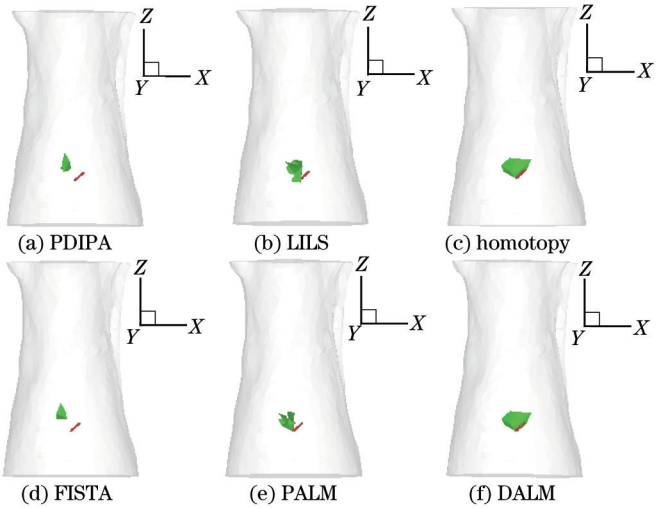

Fig.5 Reconstruction results of each algorithm in the *in vivo* experiment

4 Conclusion

We compare the performance of four kinds of typical iterative algorithms in BLT reconstruction by digital mouse experiments and *in vivo* experiments. The experimental results show that homotopy algorithm and Lagrange algorithm perform better in location accuracy. Although L1LS method is stable and suitable for large scale problem, its performance in reconstruction is not good as other algorithms. In terms of reconstruction quality, Lagrange algorithms (PALM and DALM) have relatively low power density and total power of reconstruction, but have better location accuracy. In general, homotopy method makes better performance in all indexes. Taking the sensitive analysis into account, Lagrange algorithms and homotopy algorithm are more suitable for solving the sparse BLT problem. Therefore, according to the characteristics of the algorithms in BLT reconstruction, if there is fewer measurement data in the boundary, we can use the augmented Lagrange method, which has fast computing speed and high calculation accuracy. If there is a large amount of data, we can use the homotopy method, it can guarantee both of solving speed and precision. If there is much boundary survey information, the data quantity is relatively large and the sparse degree is low, we can use interior-point methods. Due to BLT is an ill-posed problem and each method has its particular characteristics, we will pay attention to the combination of various algorithms for better performance on BLT in the future work.

References

1 Darne C, Lu Y, Sevick-Muraca E M. Small animal fluorescence and bioluminescence tomography: A review of approaches, algorithms and technology update[J]. Physics in Medicine and Biology, 2014, 59(1): R1.

2 Qin C, Feng J, Zhu S, *et al*.. Recent advances in bioluminescence tomography: Methodology and system as well as application[J]. Laser & Photonics Reviews, 2014, 8(1): 94-114.

3 Deng Dawei, Liu Fei, Cao Jie, *et al*.. Synthesis and tumor targeting research of two near-infrared fluorescence probes [J]. Chinese J Lasers, 2010, 37(11): 2735-2742.
邓大伟, 刘 飞, 曹 洁, 等. 两种近红外荧光探针的合成及肿瘤靶向研究[J]. 中国激光, 2010, 37(11): 2735-2742.

4 Li Li, Xie Wenming, Li Hui. Applications of photoacoustic spectroscopy in the field of modern biomedicine[J]. Laser & Optoelectronics Progress, 2012, 49(10): 100008.
李 莉, 谢文明, 李 晖. 光声光谱技术在现代生物医学领域的应用[J]. 激光与光电子学进展, 2012, 49(10): 100008.

5 Wang G, Cong W, Durairaj K, *et al*.. *In vivo* mouse studies with bioluminescence tomography[J]. Optics Express, 2006, 14(17): 7801-7809.

6 Cong W, Wang G. Iterative method for bioluminescence tomography based on the radiative transport equation[C]. SPIE, 2006, 6318: 631826.

7 Lv Y, Tian J, Cong W, *et al.*. A multilevel adaptive finite element algorithm for bioluminescence tomography[J]. Optics Express, 2006, 14(18): 8211-8223.

8 Jiang M, Zhou T, Cheng J, *et al.*. Image reconstruction for bioluminescence tomography from partial measurement[J]. Optics Express, 2007, 15(18): 11095-11116.

9 Chaudhari A J, Darvas F, Bading J R, *et al.*. Hyperspectral and multispectral bioluminescence optical tomography for small animal imaging[J]. Physics in Medicine and Biology, 2005, 50(23): 5421-5441.

10 Ntziachristos V, Ripoll J, Wang L V, *et al.*. Looking and listening to light: The evolution of whole-body photonic imaging[J]. Nature Biotechnology, 2005, 23(3): 313-320.

11 Tikhonov A N, Arsenin V Y. Methods for solving ill-posed problems[J]. Mathematics of Computation, 1979, 32(144): 1320-1322.

12 Gao H, Zhao H. Multilevel bioluminescence tomography based on radiative transfer equation Part 1: l_1 regularization[J]. Optics Express, 2010, 18(3): 1854-1871.

13 He X, Liang J, Wang X, *et al.*. Sparse reconstruction for quantitative bioluminescence tomography based on the incomplete variables truncated conjugate gradient method[J]. Optics Express, 2010, 18(24): 24825-24841.

14 Yu J, Liu F, Wu J, *et al.*. Fast source reconstruction for bioluminescence tomography based on sparse regularization[J]. IEEE Transactions on Biomedical Engineering, 2010, 57(10): 2583-2586.

15 Jin Chen, Guo Hongbo, Hou Yuqing, *et al.*. Research of bioluminescence tomography reconstruction problem based on simplified spherical harmonics approximation model and sparse reconstruction by separable approximation[J]. Acta Optica Sinica, 2014, 34(6): 0617001.

金 晨, 郭红波, 侯榆青, 等. 基于变量分离近似稀疏重构和简化球谐近似的生物发光断层成像[J]. 光学学报, 2014, 34(6): 0617001.

16 Potra F A, Wright S J. Interior-point methods[J]. Journal of Computational and Applied Mathematics, 2000, 124: 281-302.

17 Drori I, Donoho D L. Solution of l_1 minimization problems by LARS/homotopy methods[C]. 2006 IEEE International Conference on Acoustics, Speech and Signal Processing, 2006, 3: III.

18 d´Aspremont A, Banerjee O, Ghaoui L E. First-order methods for sparse covariance selection[J]. SIAM Journal on Matrix Analysis and Applications, 2008, 30(1): 56-66.

19 Afonso M V, Bioucas-Dias J M, Figueiredo M A T. An augmented Lagrangian approach to the constrained optimization formulation of imaging inverse problems[J]. IEEE Transactions on Image Processing, 2011, 20(3): 681-695.

20 Schweiger M, Arridge S R, Hiraoka M, *et al.*. The finite element method for the propagation of light in scattering media: Boundary and source conditions[J]. Medical Physics, 1995, 22(11): 1779-1792.

21 Wang G, Li Y, Jiang M. Uniqueness theorems in bioluminescence tomography[J]. Medical Physics, 2004, 31(8): 2289-2299.

22 Koh K, Kim S J, Boyd S. An interior-point method for large-scale l_1-regularized logistic regression[J]. Journal of Machine Learning Research, 2007, 8(8): 1519-1555.

23 Efron B, Hastie T, Johnstone I, *et al.*. Least angle regression[J]. The Annals of Statistics, 2004, 32(2): 407-499.

24 Bertsekas D P. Nonlinear Programming[M]. Nashua: Athena Scientific, 1999.

25 Alexandrakis G, Rannou F R, Chatziioannou A F, *et al.*. Tomographic bioluminescence imaging by use of a combined optical-PET (OPET) system: A computer simulation feasibility study[J]. Physics in Medicine and Biology, 2005, 50(17): 4225-4241.

栏目编辑：吴秀娟